Quantification of blood-flow dependent component in estimates of beta-amyloid load obtained using quasi-steady-state standardized uptake value ratio

Zsolt Cselényi, MD PhD[1,2]; Lars Farde, MD PhD[1,2] and for the Alzheimer's Disease Neuroimaging Initiative[3]

[1]*PET Centre, Department of Clinical Neuroscience, Karolinska Institutet, Stockholm, Sweden*

[2]*AstraZeneca Translational Science Centre at Karolinska Institutet, Stockholm, Sweden*

[3]*Data used in preparation of this article were obtained from the Alzheimer's Disease Neuroimaging Initiative (ADNI) database (adni.loni.usc.edu). As such, the investigators within the ADNI contributed to the design and implementation of ADNI and/or provided data but did not participate in analysis or writing of this report. A complete listing of ADNI investigators can be found at: http://adni.loni.usc.edu/wp-content/uploads/how_to_apply/ADNI_Acknowledgement_List.pdf*

Supplementary Material

PET Image Pre-processing

Figure S1. Flow-chart of PET image pre-processing steps performed in ADNI and additional ones in the present work. Boxes with wavy lower edge indicate PET data (4D PET data shown as a stack of such boxes), rounded boxes indicate processing steps and skewed boxes indicate parameters for processing. Naming of PET data is according to ADNI nomenclature even for processed data obtained in the present work. PET data available in the ADNI database are marked using thick-edged boxes, even if data-set has been recalculated in the present work. Processing steps done in ADNI, along with parameters applied there, are marked using thin, dashed edges and arrows. Processing steps performed in the present work are marked with bold font and numbering that matches that in the manuscript methods section, and with thick connecting arrows between the boxes. Parameters and data-sets obtained in the present work are also indicated using bold font.

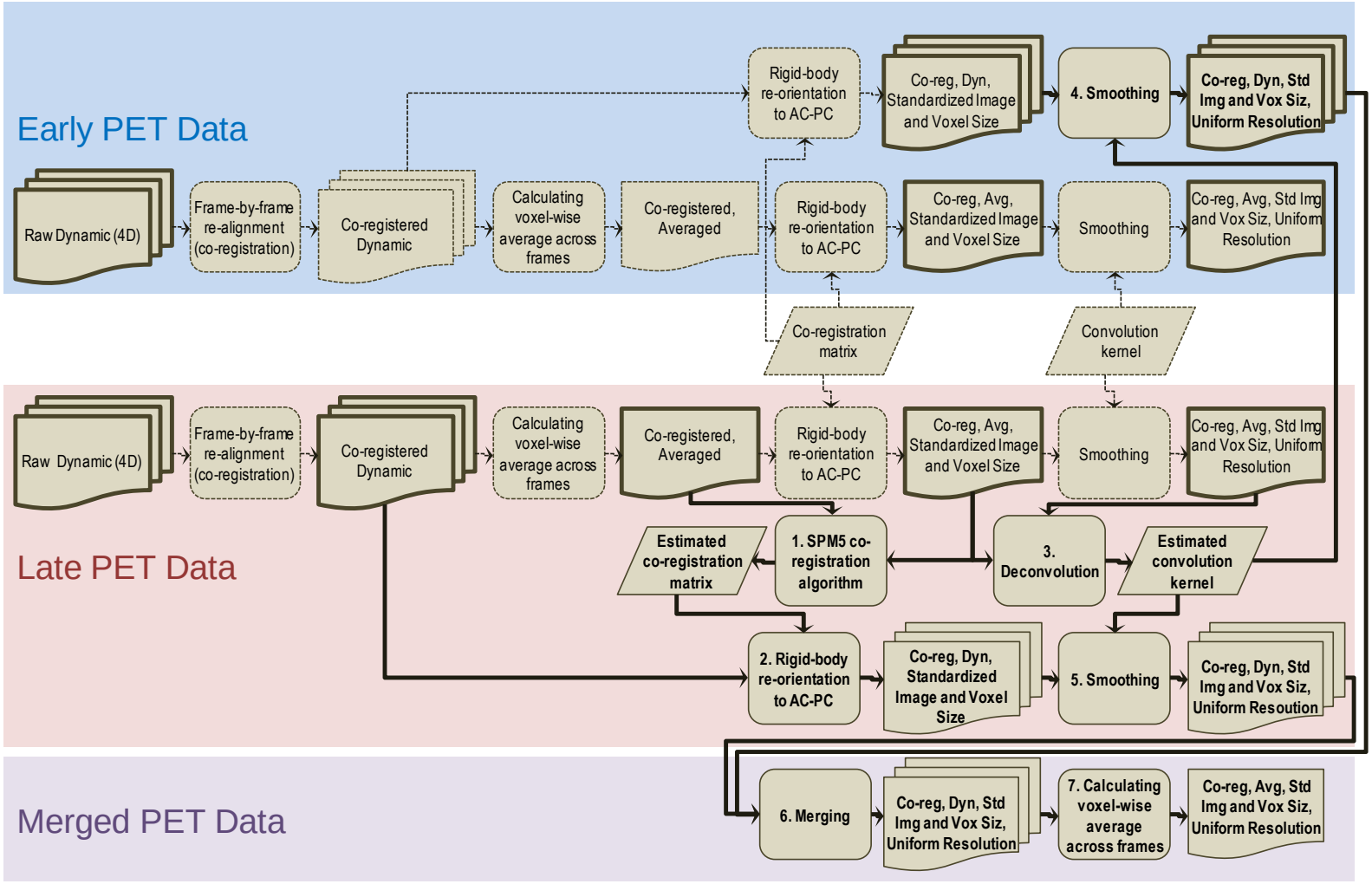

Additional analyses using alternatively defined reference and target regions and applying partial volume effect correction

Methods

Three additional analyses were performed. In the first two cases the reference region comprised the whole cerebellum, i.e. including both grey and white matter dominated voxels. This whole cerebellum region was defined in MNI space by adding to the mask of the AAL cerebellar template all white matter voxels in cerebellum (Fig. S2).

Figure S2. Orthographic projections showing the whole cerebellar template mask overlaid on a T1-weighted MRI provided in the SPM package to represent standard brain anatomy in MNI space.

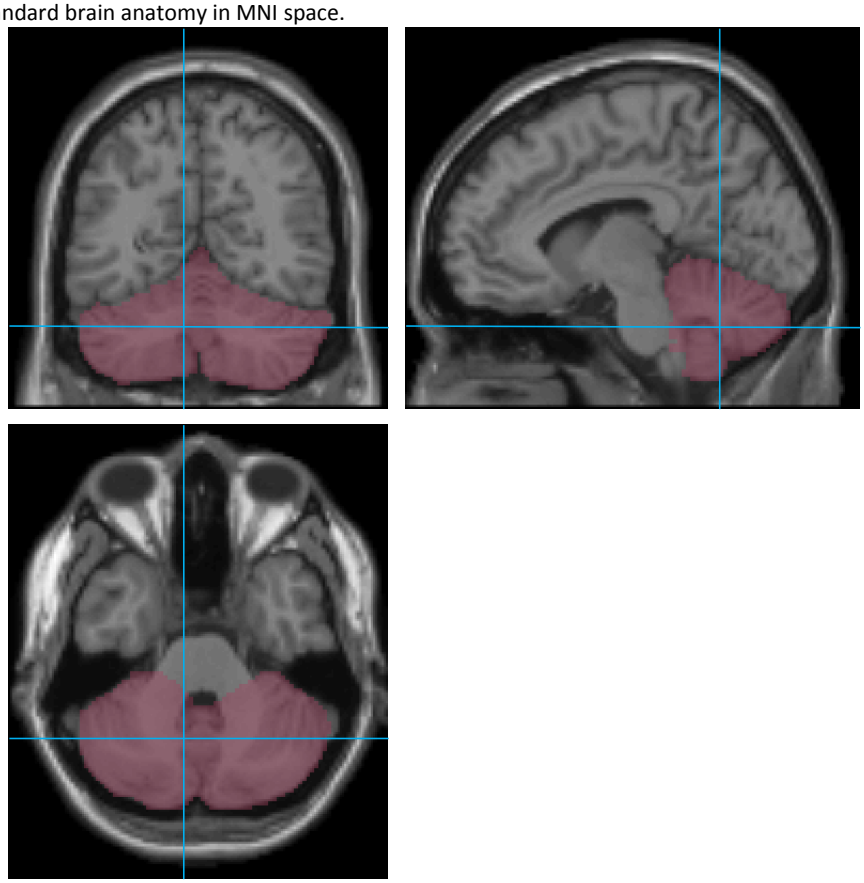

The first additional analysis omitted the use of grey matter (GM) segmentation in the target regions so that white matter dominant voxels were also included in these regions. The second analysis retained the use of grey matter segmentation, i.e. the same TACs were used as in the main analysis. In all other respects the additional analyses were performed in a way identical to that described in the main body of the article.

The third additional analysis used the same reference region (cerebellar cortex) as the main analysis. Instead it employed additional target regions in a way that all the AAL template defined regions were included. The additional bi-lateral regions were: sensorimotor cortex (consisting of AAL regions FA, PA, OR), medial frontal

cortex (AAL regions FM, SMA, LPC), orbitofrontal cortex (AAL regions F1O, FMO, F2O, F3O, GR, COB), medial temporal cortex (AAL region FUSI), lateral parietal cortex (AAL regions P1, P2, GA, GSM), lateral occipital cortex (AAL regions O1, O2, O3), medial inferior occipital cortex (AAL regions Q, V1, LING), temporal pole (AAL regions T1A, T2A), median cingulate cortex (AAL region CINM), hippocampus (AAL region HIPPO), parahippocampus (AAL region PARA_HIPPO), insula (AAL region IN), amygdala (AAL region AMYGD), caudate nucleus (AAL region NC), putamen (AAL region NL), pallidum (AAL region PALL), and thalamus (AAL region THA). Grey matter trimming was performed in each cortical ROI but not in case of subcortical nuclei. Additionally, a bi-lateral white matter ROI was defined automatically. First voxels with higher than 50% probability on the white matter segmentation image (in MR space) were retained in a binary mask then this mask was eroded and finally only those mask voxels were retained that belonged to the 6 axially adjacent planes containing most in-mask voxels (typically in area of centrum semiovale). The full set of ROIs thus obtained was used in a geometric transfer function (GTM) based partial volume effect (PVE) correction scheme as described earlier (see ref. 32 in main article) to obtain corrected TACs. For this the 4D PET image was first resliced to the orientation and 1 mm isotropic voxel size of the MR image using the inverse of the co-registration matrix described in the main analysis. A point spread function of 8 mm full-width at half maximum was used in the PVE correction scheme since all PET images were harmonized to this resolution in the pre-processing. The DVR, R_1, $SUVR_{50\text{-}70}$ quantification and TLS regression in the third additional analysis was performed using the corrected TACs but otherwise in the same way as described in the main analysis.

The typical "healthy" cortical R_1 value can be influenced by choice and handling of reference and target regions. Therefore in order to calculate the flow component in $SUVR_{50\text{-}70}$ in the additional analyses, the average R_1 value in the cognitively normal (CN) group (R_{1_CN}) was used in place of unity (see Eg. 3 in main article). In detail, the flow-dependent component was here calculated as:

$$\text{Flow component in } \mathbf{SUVR_{50-70}} = b_2 \times \left(\mathbf{R_1} - \mathrm{R}_{1\_\mathrm{CN}}\right) = b_2 \times \mathbf{R_1} - b_2 \qquad \text{Eq. S1}$$

, i.e. considering the effect of the relative blood-flow deviating from average R_1 in CN.

Analogously, the "flow-corrected" $SUVR_{50\text{-}70}$ ($FCSUVR_{50\text{-}70}$) was calculated as:

$$\mathrm{FCSUVR}_{50-70} = \mathrm{SUVR}_{50-70} - b_2 \times \left(\mathbf{R_1} - \mathrm{R}_{1\_\mathrm{CN}}\right) \qquad \text{Eq. S2}$$

, which is equivalent to:

$$\mathrm{FCSUVR}_{50-70} = b_1 \times \mathbf{DVR} + b_2 \times \mathrm{R}_{1\_\mathrm{CN}} + b_3 + \varepsilon_3 \qquad \text{Eq. S3}$$

Results

The regression results of the first additional analysis, omitting GM segmentation in both reference and target regions, are presented in Table S1 and Fig. S3. The dynamic range of $SUVR_{50-70}$ values across subjects with varying amount of amyloid was narrower than in the main analysis. The R_1 values were overall lower than in the main analysis. The multivariate TLS indicated a significant negative slope along the R_1 axis.

Table S1. Results of total least squares analyses. Input region: whole cerebellum. Target regions: without GM segmentation

Variables	Equation for fitted line or plane	TLS parameter estimates (with 95% confidence limits)			
$SUVR_{50-70}$, DVR	$SUVR_{50-70}=b_1 \times DVR+b_2$	b_1 =	1.59	[1.51;	1.69]
		b_2 =	-0.50	[-0.61;	-0.40]
$SUVR_{50-70}$, R_1	$SUVR_{50-70}=b_1 \times R_1+b_2$	b_1 =	-25.63	[-1024.72;	47.58]
		b_2 =	25.27	[-43.31;	950.54]
$SUVR_{50-70}$, DVR, R_1	$SUVR_{50-70}=b_1 \times DVR+b_2 \times R_1+b_3$	b_1 =	1.58	[1.50;	1.66]
		b_2 =	-0.40	[-0.61;	-0.23]
		b_3 =	-0.10	[-0.27;	0.09]

Figure S3. Regression of global cortical $SUVR_{50-70}$ values against estimates of amyloid and relative flow, respectively (N=101). Input region: whole cerebellum. Target regions: without GM segmentation. For illustration purposes subjects with high and low amyloid load were separated as in the main analysis. Individual symbols indicate group membership and amyloid positivity (see legend for details). Solid line shows total least-squares fitted line (equation in legend, together with results of simple linear correlation). A. $SUVR_{50-70}$ values vs. amyloid binding estimates (DVR). B. $SUVR_{50-70}$ values vs. relative blood flow estimates (R_1). Vertical dashed line indicates average R_1 in CN. C. $SUVR_{50-70}$ values after removing flow-dependent component (FCSUVR) vs. amyloid binding estimates (DVR). D. $SUVR_{50-70}$ values after removing amyloid-dependent component (ACSUVR) vs. relative blood flow estimates (R_1). Vertical dashed line indicates average R_1 in CN.

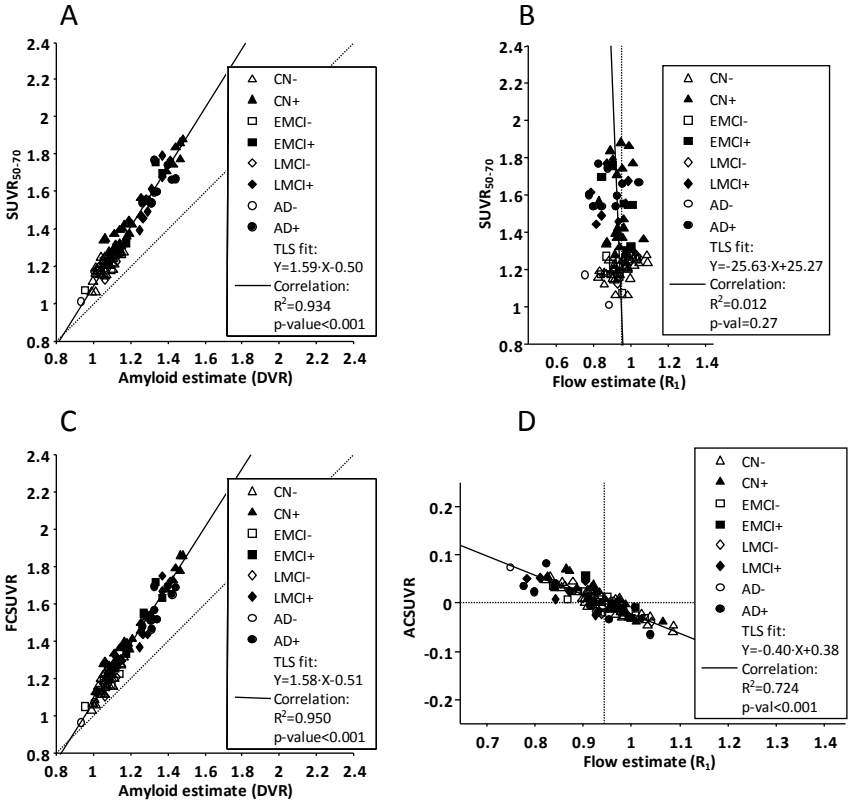

The regression results of the second additional analysis, retaining GM segmentation in target regions but not in the reference region, are presented in Table S2 and Fig. S4. Unlike in the first additional analysis, the R_1 values were slightly higher than those in the main analysis. On the other hand, similarly to the first additional analysis, the dynamic range of $SUVR_{50\text{-}70}$ values was narrower than in the main analysis and the multivariate TLS indicated a significant negative slope along the R_1 axis.

Table S2. Results of total least squares analyses. Input region: whole cerebellum. Target regions: with GM segmentation

Variables	Equation for fitted line or plane	TLS parameter estimates (with 95% confidence limits)			
$SUVR_{50\text{-}70}$, DVR	$SUVR_{50\text{-}70}=b_1\times DVR+b_2$	b_1 =	1.58 [	1.51;	1.66]
		b_2 =	-0.53 [	-0.61;	-0.46]
$SUVR_{50\text{-}70}$, R_1	$SUVR_{50\text{-}70}=b_1\times R_1+b_2$	b_1 =	-17.66 [	-158.47;	17.07]
		b_2 =	18.89 [	-19.33;	159.34]
$SUVR_{50\text{-}70}$, DVR, R_1	$SUVR_{50\text{-}70}=b_1\times DVR+b_2\times R_1+b_3$	b_1 =	1.56 [	1.50;	1.63]
		b_2 =	-0.34 [	-0.46;	-0.23]
		b_3 =	-0.16 [	-0.29;	-0.03]

Figure S4. Regression of global cortical $SUVR_{50\text{-}70}$ values against estimates of amyloid and relative flow, respectively (N=101). Input region: whole cerebellum. Target regions: with GM segmentation. For illustration purposes subjects with high and low amyloid load were separated as in the main analysis. Individual symbols indicate group membership and amyloid positivity (see legend for details). Solid line shows total least-squares fitted line (equation in legend, together with results of simple linear correlation). A. $SUVR_{50\text{-}70}$ values vs. amyloid binding estimates (DVR). B. $SUVR_{50\text{-}70}$ values vs. relative blood flow estimates (R_1). Vertical dashed line indicates average R_1 in CN. C. $SUVR_{50\text{-}70}$ values after removing flow-dependent component (FCSUVR) vs. amyloid binding estimates (DVR). D. $SUVR_{50\text{-}70}$ values after removing amyloid-dependent component (ACSUVR) vs. relative blood flow estimates (R_1). Vertical dashed line indicates average R_1 in CN.

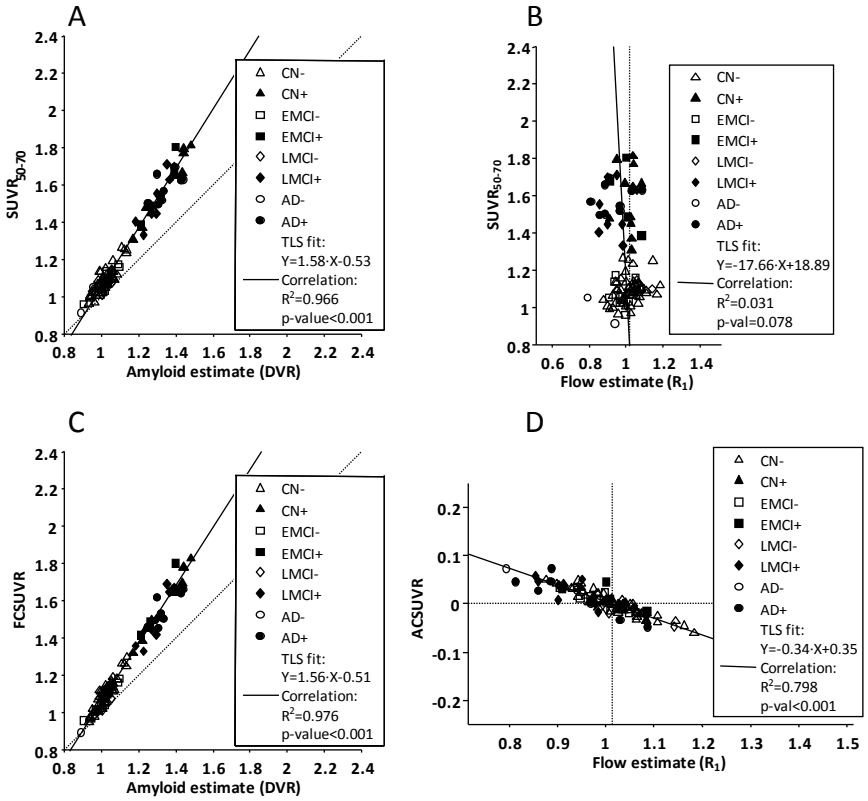

The regression results of the third additional analysis, based on PVE corrected TACs in both target and reference regions, are presented in Table S3 and Fig. S5. The R_1 values were higher than those in all the other analyses. Also the dynamic range of all 3 parameters was wider than in the other analyses: most for $SUVR_{50\text{-}70}$, followed by DVR and then R_1. The multivariate TLS indicated a significant negative slope along the R_1 axis that was almost twice as steep as that in the main analysis.

Table S3. Results of total least squares analyses. Input region: cerebellar cortex. Both target and reference regions with GM segmentation and PVE correction

Variables	Equation for fitted line or plane	TLS parameter estimates (with 95% confidence limits)			
$SUVR_{50\text{-}70}$, DVR	$SUVR_{50\text{-}70}=b_1\times DVR+b_2$	b_1 =	2.04 [	1.93;	2.18]
		b_2 =	-1.33 [	-1.52;	-1.19]
$SUVR_{50\text{-}70}$, R_1	$SUVR_{50\text{-}70}=b_1\times R_1+b_2$	b_1 =	-28.89 [	-168.40;	-11.78]
		b_2 =	38.49 [	16.51;	217.13]
$SUVR_{50\text{-}70}$, DVR, R_1	$SUVR_{50\text{-}70}=b_1\times DVR+b_2\times R_1+b_3$	b_1 =	1.98 [	1.88;	2.09]
		b_2 =	-0.83 [	-1.32;	-0.50]
		b_3 =	-0.20 [	-0.62;	0.41]

Figure S5. Regression of global cortical $SUVR_{50\text{-}70}$ values against estimates of amyloid and relative flow, respectively (N=101). Input region: cerebellar cortex. Both target and reference regions with GM segmentation and PVE correction. For illustration purposes subjects with high and low amyloid load were separated as in the main analysis. Individual symbols indicate group membership and amyloid positivity (see legend for details). Solid line shows total least-squares fitted line (equation in legend, together with results of simple linear correlation). A. $SUVR_{50\text{-}70}$ values vs. amyloid binding estimates (DVR). B. $SUVR_{50\text{-}70}$ values vs. relative blood flow estimates (R_1). Vertical dashed line indicates average R_1 in CN. C. $SUVR_{50\text{-}70}$ values after removing flow-dependent component (FCSUVR) vs. amyloid binding estimates (DVR). D. $SUVR_{50\text{-}70}$ values after removing amyloid-dependent component (ACSUVR) vs. relative blood flow estimates (R_1). Vertical dashed line indicates average R_1 in CN.

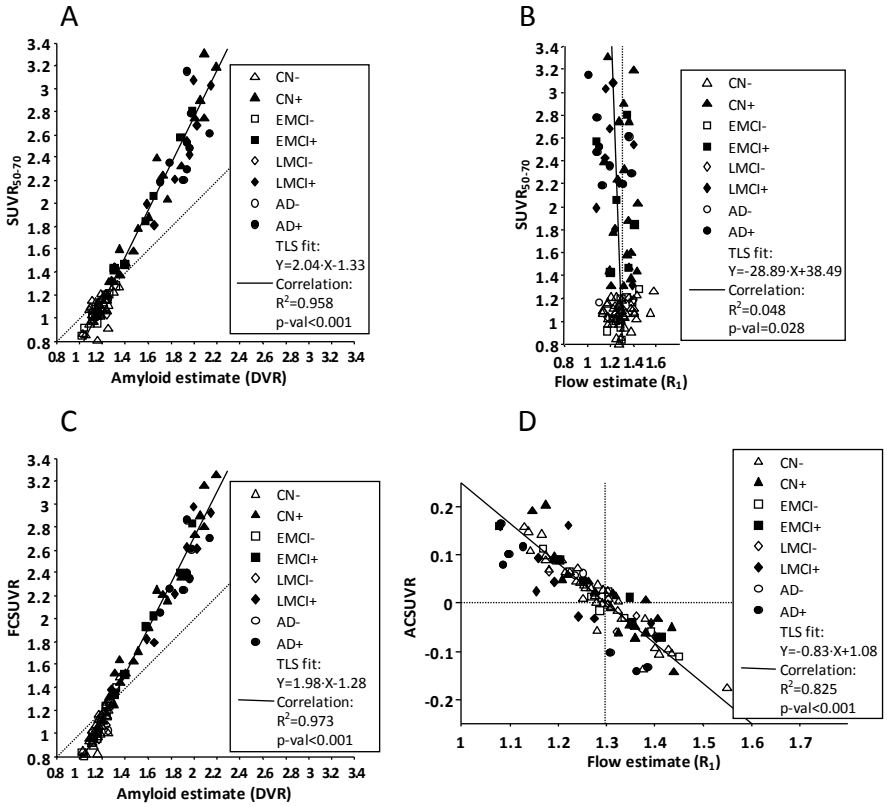

In the first additional analysis, the extracted flow-dependent components in $SUVR_{50-70}$ were overall slightly closer to zero compared to the main analysis (Fig. S6A). On average the AD group had the highest component (mean±SD=0.025±0.035, N=12), followed by LMCI (mean±SD=0.008±0.031, N=13) with values near zero in EMCI (mean±SD=0.003±0.024, N=16) and at zero in CN (mean±SD=0.000±0.024, N=60). The mean blood-flow-dependent effect was different in an uncorrected multiple comparison at the α=5% level between AD and EMCI (p-value: 0.049), and between AD and CN (p-value: 0.0033), respectively (two-sided, two sample t-test). Performing an ANOVA indicated an overall group effect at the α=5% level (p-value: 0.031) and a Scheffé-multiple comparison procedure indicated a retained significant group difference between AD and CN.

In the second additional analysis, the extracted flow-dependent components were overall close to those in the main analysis (Fig. S6B). On average the AD group had the highest component (mean±SD=0.028±0.031, N=12), followed by LMCI (mean±SD=0.010±0.030, N=13) with values close to zero in EMCI (mean±SD=0.004±0.020, N=16) and at zero in CN (mean±SD=0.000±0.022, N=60). The mean blood-flow-dependent effect was different in an uncorrected multiple comparison at the α=5% level between AD and EMCI (p-value: 0.022), and between AD and CN (p-value: 0.0004), respectively (two-sided, two sample t-test). Performing the ANOVA indicated an overall group effect at the α=5% level (p-value: 0.004) and the Scheffé-multiple comparison procedure indicated a retained significant group difference between AD and CN.

In the third additional analysis, the extracted flow-dependent components were overall larger than in the main analysis (Fig. S6C). On average the AD group had the highest component (mean±SD=0.080±0.113, N=12), followed by LMCI (mean±SD=0.025±0.083, N=13) with values close to zero in EMCI (mean±SD=0.014±0.077, N=16) and CN (mean±SD=0.003±0.080, N=60). The mean blood-flow-dependent effect was different in an uncorrected multiple comparison at the α=5% level between AD and CN (p-value: 0.006), respectively (two-sided, two sample t-test). Performing the ANOVA indicated an overall group effect at the α=5% level (p-value: 0.042) and the Scheffé-multiple comparison procedure indicated a retained significant group difference between AD and CN.

Figure S6. Box plots of flow-dependent component in $SUVR_{50-70}$ in the four subject groups: CN, EMCI, LMCI and AD. The grey boxes indicate the upper and lower quartiles, the black lines in the boxes show the median, the black × marker the mean and the whiskers indicate the minimum and maximum values. Individual data points are also plotted with open symbols showing amyloid negativity and filled symbols indicating amyloid positivity. Points are randomly shifted horizontally to decrease visual clutter. Significant group differences are indicated above the plot with the corresponding p-value cut-off (two-tailed, two-sample t-test). A. Input region: whole cerebellum. Target regions: obtained without GM segmentation. B. Input region: whole cerebellum. Target regions: obtained with GM segmentation. C. Input region: cerebellar cortex. Both target and reference regions with GM segmentation and PVE correction.

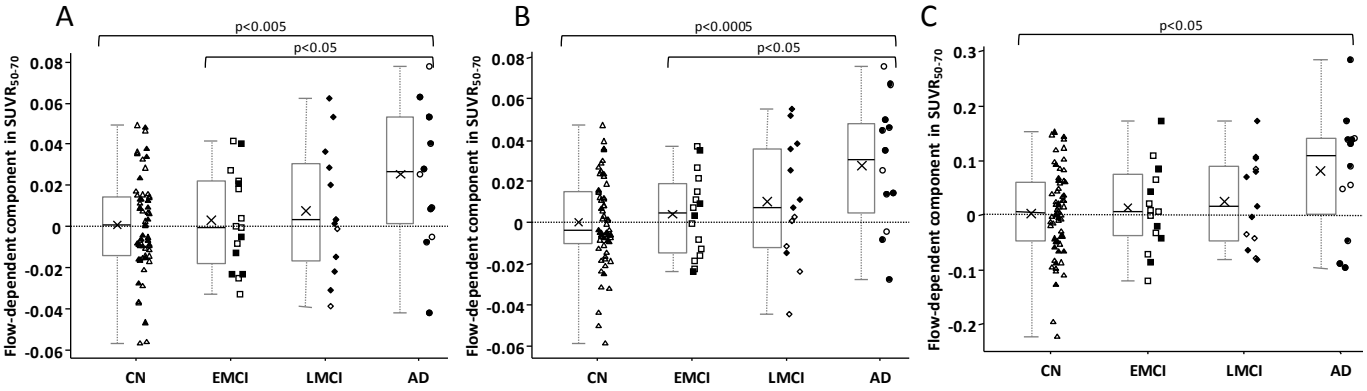

Discussion

In the first two additional analyses, as expected, using more white matter dominated voxels in the reference region yielded DVR and $SUVR_{50-70}$ values with less dynamic range. The results also demonstrated that using more white-matter voxels in the reference (e.g. whole cerebellum, brainstem, etc.) or target regions can affect the typical expected ("normative") R_1 value in healthy tissue (i.e. it is greater than 1.0 if the reference and less than 1.0 if the target region has relatively more white matter voxels). Correcting for PVE in the third additional analysis demonstrated that the true dynamic range of all three parameters is larger, especially that of $SUVR_{50-70}$. The typical R_1 value was above 1, indicating that PVE correction has more corrective effect in cerebral cortex possibly because the finely detailed grey-white matter relationship in the cerebellum (arbor vitae) cannot be sufficiently handled using MR images with approx. 1 mm resolution so there is still some remaining PVE in the cerebellar cortical TACs.

Compared to the main analysis the multivariate TLS fit provided somewhat different slopes both along the axis of blood flow and that of amyloid with markedly steeper slopes in case of the third additional analysis based on PVE correction. However, in all cases the basic relationship and significant blood flow dependency remained with a negative slope along the R_1 axis and similar group differences. Thus the implications and the final conclusions appear to be essentially the same as in the main analysis irrespective of choice of reference region, method of segmenting the target regions or use of PVE correction.